The Impact of Lignin Biopolymer Sources, Isolation, and Size Reduction from the Macro- to Nanoscale on the Performances of Next-Generation Sunscreen

Victor Girard, Léane Fragnières, Hubert Chapuis, Nicolas Brosse, Laurent Marchal-Heussler, Nadia Canilho, Stéphane Parant, Isabelle Ziegler-Devin

polymers

MDPI

Article

The Impact of Lignin Biopolymer Sources, Isolation, and Size Reduction from the Macro- to Nanoscale on the Performances of Next-Generation Sunscreen

Victor Girard [1,*], Léane Fragnières [1], Hubert Chapuis [1], Nicolas Brosse [1], Laurent Marchal-Heussler [2], Nadia Canilho [3], Stéphane Parant [3] and Isabelle Ziegler-Devin [1]

[1] Laboratoire d'Etude et de Recherche sur le MAtériau Bois (LERMAB), Faculty of Science and Technology, University of Lorraine, F-54000 Nancy, France; leane.fragnieres@etu.unistra.fr (L.F.); hubert.chapuis@univ-lorraine.fr (H.C.); nicolas.brosse@univ-lorraine.fr (N.B.); isabelle.ziegler@univ-lorraine.fr (I.Z.-D.)

[2] Ecole Nationale Supérieure des Industries Chimique (ENSIC), University of Lorraine, F-54000 Nancy, France; laurent.marchal-heussler@univ-lorraine.fr

[3] Laboratoire Lorrain de Chimie Moléculaire (L2CM), Faculty of Science and Technology, University of Lorraine, F-54000 Nancy, France; nadia.canilho@univ-lorraine.fr (N.C.); stephane.parant@univ-lorraine.fr (S.P.)

* Correspondence: victor.girard@univ-lorraine.fr

Abstract: In recent years, concerns about the harmful effects of synthetic UV filters on the environment have highlighted the need for natural sun blockers. Lignin, the most abundant aromatic renewable biopolymer on Earth, is a promising candidate for next-generation sunscreen due to its inherent UV absorbance and its green, biodegradable, and biocompatible properties. Lignin's limitations, such as its dark color and poor dispersity, can be overcome by reducing particle size to the nanoscale, enhancing UV protection and formulation. In this study, 100–200 nm lignin nanoparticles (LNPs) were prepared from various biomass by-products (hardwood, softwood, and herbaceous material) using an eco-friendly anti-solvent precipitation method. Pure lignin macroparticles (LMPs) were extracted from beech, spruce, and wheat straw using an ethanol–organosolv treatment and compared with sulfur-rich kraft lignin (KL). Sunscreen lotions made from these LMPs and LNPs at various concentrations demonstrated novel UV-shielding properties based on biomass source and particle size. The results showed that transitioning from the macro- to nanoscale increased the sun protection factor (SPF) by at least 2.5 times, with the best results improving the SPF from 7.5 to 42 for wheat straw LMPs and LNPs at 5 wt%. This study underscores lignin's potential in developing high-quality green sunscreens, aligning with green chemistry principles.

Keywords: lignin; sunscreens; lignin nanoparticles; organosolv; UV shielding; eco-friendly production

Citation: Girard, V.; Fragnières, L.; Chapuis, H.; Brosse, N.; Marchal-Heussler, L.; Canilho, N.; Parant, S.; Ziegler-Devin, I. The Impact of Lignin Biopolymer Sources, Isolation, and Size Reduction from the Macro- to Nanoscale on the Performances of Next-Generation Sunscreen. *Polymers* **2024**, *16*, 1901. https://doi.org/10.3390/polym16131901

Academic Editor: Rossella Arrigo

Received: 29 May 2024
Revised: 22 June 2024
Accepted: 1 July 2024
Published: 2 July 2024

1. Introduction

In a world where the growing concerns of environmental sustainability and improved ultraviolet (UV) radiation levels caused by ozone layer depletion due to human activity converge, the development of sunscreens that are both eco-friendly and effective in shielding against harmful UV radiation has become an increasingly pressing challenge.

Sunburn, skin damage, or the potential development of cancer can be attributed to prolonged UVB (290–320 nm) exposure compared to less energetic UVA (320–400 nm) [1,2]. In response to these concerns, traditional commercial sunscreen has relied on contentious organic and inorganic UV filters [3], such as titanium dioxide [4] (TiO_2), to protect human skin from UV rays despite significant apprehensions, including high environmental impact and persistence [5], skin sensitivities, and limited UV protection spectrum [6].

As an example, it has recently been proven that common chemical or physical UV absorbers, such as ZnO, TiO_2, oxybenzone, octocrylene, or octinoxate, are responsible for marine ecosystem modification [7] and coral bleaching [8,9]. This prompted Australia and Hawaii [7,10] to prohibit these UV-active components with respect to the annual 14,000 tons [11] of sunscreen that end up in the world's oceans [12].

In this context, lignin—the most abundant aromatic biopolymer [13–16] constituting 30% of the non-fossil organic carbon in nature [17,18] with proven high UV absorption [19–31] and low cytotoxicity [32–37]—presents tremendous potential for next-generation sunscreens. Lignin's complex polymer structure contains phenylpropane units composed of guaiacyl (G), syringyl (S), and p-hydroxypenyl (H) monomeric units linked by aryl ether and carbon–carbon bonds (Figure 1) [38,39]. Furthermore, lignin's UV-absorbing properties are related to functional groups, such as phenolic, quinones, and methoxy substituted groups, and other chromophores [40–43], making this sustainable polymer an excellent absorber in the UVB–UVA wavelength areas targeted by a wide range of sunscreens [12].

Annually, 50 million tons of generated lignin is used as an energy source [44–46]. Despite its great potential, lignin is seldom used for non-energy applications due to processing challenges [47], the inherent heterogeneity of the macromolecular structure depending on isolation methods and biomass nature [48], and particles that are too large, limiting industrial applications. Currently, lignin studies and valorizations are mainly focused on technical lignin materials [49], such as lignosulfonate or kraft lignin (KL), regardless of environmental limitations [50,51] and the presence of sulfur [17,52], which immediately hinders many possible uses, such as cosmetics [53].

However, lignin biopolymers could take advantage of novel eco-friendly isolation processes, similar to organosolv [51], and they can also take advantage of the emerging integration of nanotechnology in cosmetics to address current limitations. Precisely, the extensive reach of nanotechnology in the cosmetic industry, as observed in inorganic ZnO and TiO_2 UV filters, results from the enhanced properties of nanoparticles, including their size, stability, shape, reactivity, color, or solubility [54]. Recent studies showed that lignin's inherent heterogeneity, dark color, and poor dispersibility could be overcome thanks to particle size reduction [26], while maintaining a size of over 45 nm to avoid skin absorption risks [55] and meet the Scientific Committee on Consumer Safety (SCCS) marketing requirements. For example, Qian et al. [22] showed that the sun protection factor (SPF) of mixed sunscreens with lignin is boosted according to particle size reduction.

Various methods, such as nano-precipitation [56–62], mechanical and ultrasound treatments [63–67], or aerosol processing [68], have been investigated for producing lignin nanoparticles (LNPs) with linked properties (size, shape, stability, and reactivity) [69]. However, previous studies predominantly used kraft lignin, without consistently specifying the biomass source or thoroughly examining the production yields and the actual impact of particle size reduction on UV-absorbing properties. This limitation results in an incomplete understanding of the value of lignin potential for next-generation sunscreen.

Knowing that the organosolv isolation process produced higher UV-shielding lignin compared to other extraction methods, as demonstrated by Qian et al. [20] and Tan et al. [70], this study employed, for the first time, a global sustainable method from various biomass by-products using only ethanol, water, and heat for pure lignin macroparticles (LMPs) extraction via organosolv pretreatment (OL) and particle size reduction (nano-precipitation). This new top-down lignin-based approach, described for the first time by Girard et al. [71], allowed the production of different eco-friendly concentrated LNPs suspensions with improved characteristics while having high production yields. Then, LMPs and LNPs-based formulations were developed to highlight the size reduction in UV-absorbing properties with respect to used pure cream and sunscreen. As lignin's UV-absorbing properties are related to its chemical structure (assessed via SEC and HSQC and ^{31}P NMR), which varies according to the feedstock source, the prepared sunscreens with different inputs (hardwood, softwood, and grasses) and lignin types (KL and OL) were

analyzed to determine the most suitable lignin chemical structure for UV absorption. The performance of lignin-based formulations was compared to that of commercial SPF 10 and SPF 30 sunscreens containing TiO_2 nanoparticles in order to assess the commercialization potential of lignin-based formulations.

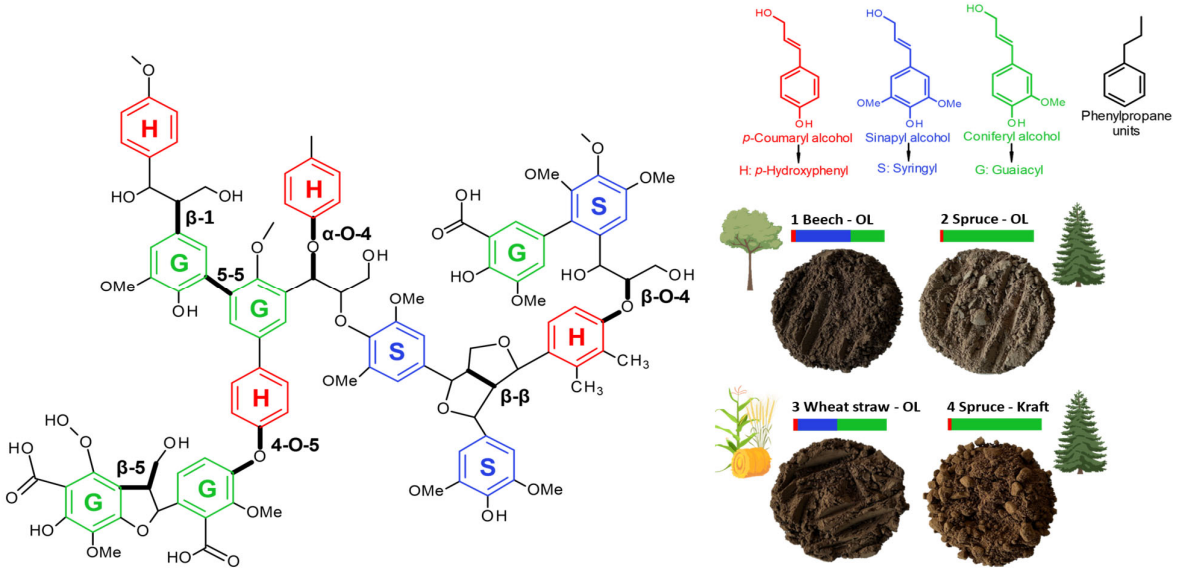

Figure 1. Lignin chemical structure with the main linkages and the proportion of different monolignols and monomeric units (G, S, and H) according to the biomass source. Photographs of the organosolv (OL)-extracted lignin's with beech (1), spruce (2), and wheat straw (3). Comparison with kraft lignin (KL) from spruce (4).

2. Materials and Methods

2.1. Raw Materials

Commercial kraft lignin was provided by the Lineo™ Prime W by Stora Enso process (CAS Number 8068-05-1, Kotka, Finland). Organosolv (OL) lignin was extracted from three distinct and local biomass by-products from Vosges forests and meadows (Epinal, France). Selected by-products included beech (*Fagus sylvatica*), spruce (*Picea abies* L.), and wheat straw (*Triticum*) provided by the French National School of Wood Technologies and Timber Engineering (ENSTIB, Épinal, France) and the "Bergerie de Straiture" sheepfold (Ban-Sur-Meurthe-Clefcy, France). NIVEA® Soft moisturizing skin care cream (200 mL, Hambourg, Germany) (Art.-No. 89050) was used as the basis for the formulation of sunscreen; this cream is mentioned as "pure cream" hereafter. Sunscreen lotion comprised GARNIER® Latte protettivo SPF 10 (200 mL, Loudéac, France) and CIEN® Sun SPF 30 (75 mL, Paris, France). Cream and sunscreen were purchased from European drug markets.

2.2. Biomass Chemical Characterization

Chemical composition analysis, following the National Renewable Energy Laboratory (NREL) labeling protocols and TAPPI method T222, was conducted on biomass powder. The procedure involved ash content determination (NREL/TP-510-42622), Soxhlet extraction (NREL/TP-510-42619), and analyses of acid-insoluble lignin and monomeric sugar contents from free extractive biomass (NREL/TP-510-42618 and TP-510-42623). High-performance anion exchange chromatography coupled with pulsed amperometry detection (HPAE-PAD, ICS-3000 Dionex®, Sunnyvale, California, United States) was employed for monomeric sugar analyses (CarboPac PA-20 Dionex® analytical column). The composition's gradient involved ultrapure water and 250 mM NaOH solutions eluted at 35 °C and 0.4 mL/min. Fucose, arabinose, rhamnose, galactose, glucose, xylose, mannose,

galacturonic acid, and glucuronic acid were determined via external calibration (Sigma-Aldrich, St Louis, Missouri, United States). Chemical content comprised the following: (1) beech: extractives = 2.67 ± 0.27 (%, *w*/*w*), cellulose = 47.80 ± 1.47 (%, *w*/*w*), hemicelluloses = 22.52 ± 0.86 (%, *w*/*w*), lignin = 23.70 ± 0.25 (%, *w*/*w*), and ashes 0.73 ± 0.01 (%, *w*/*w*); (2) spruce: extractives = 2.14 ± 0.24 (%, *w*/*w*), cellulose = 45.06 ± 1.19 (%, *w*/*w*), hemicelluloses = 21.41 ± 1.19 (%, *w*/*w*), lignin = 27.86 ± 0.33 (%, *w*/*w*), and ashes 0.36 ± 0.01 (%, *w*/*w*); (3) wheat straw: extractives = 0.56 ± 0.15 (%, *w*/*w*), cellulose = 49.56 ± 1.05 (%, *w*/*w*), hemicelluloses = 23.21 ± 0.69 (%, *w*/*w*), lignin = 20.52 ± 0.24 (%, *w*/*w*), and ashes 6.34 ± 0.07 (%, *w*/*w*).

2.3. Lignin Macroparticles (LMPs) Extraction

Macroscale lignin from local biomass was obtained by employing OL treatment. For this purpose, biomass was first coarsely crushed into ø8 mm particles with a Retsch® cross beater mill SK100 (Düsseldorf, Germany) prior to the OL extraction process. In a pressurized PARR® 4568 2-L benchtop reactor (Moline, Illinois, United States), 100 g of dry biomass underwent 1 h treatment at 200 °C in a 60/40 *v*/*v* EtOH/H_2O solution, maintaining a liquid–solid ratio of 10/1. The reactor was then quickly cooled in an ice bath to stop the chemical reaction. Extracted black liquor was separated from the solid phase through vacuum filtration. The lignin contained in the black liquor mixture was isolated via direct precipitation with cold distilled water at a 1/3 *v*/*v* ratio. After 1 h, the precipitated lignin was filtered via vacuum filtration using a 1.6 µm glass macrofibre filter. Finally, the separated lignin was washed with 500 mL of distilled water before drying in a controlled oven at 40 °C for 2 days. LMPs powder was stored in a dark room before further analyses. The milled wood lignin (MWL) extraction method is based on preliminary findings from our research group [72].

2.4. Lignin Nanoparticles (LNPs) Preparation

LNPs were synthesized through a simple, environmentally friendly anti-solvent precipitation method. Initially, each LMPs fraction was dissolved in an 80% *v*/*v* EtOH/H_2O solution with ultrasonic treatment for 1 h to ensure complete lignin solubilization at a concentration of 30 mg/mL. The resulting solution sustained vacuum filtration using a 0.45 µm nylon filter to eliminate potential aggregates, which represented between 0.9 and 3.1% of the total solubilized mass for beech, spruce, and wheat straw compared with 6.8% for KL. The production of LNPs is performed thanks to the addition of the LMPs solution to the anti-solvent phase with a KF Technology® NE-1010 (Roma, Italy) syringe pump. Each phase is kept at 20 °C, and the addition of the LMPs phase is performed under magnetic stirring (500 rpm) at a constant flow rate of 100 mL/min until achieving a final concentration of 3 mg/mL. The resulting LNPs suspensions were predominantly aqueous, with a composition of 91/9 H_2O/EtOH *v*/*v*. Suspensions were stored at 4 °C and further freeze-dried for 48 h using a BILON® FD-1A-50 freeze dryer (Beijing, China) to obtain dried LNPs.

2.5. Elemental Analysis

Thermo Finnigan Flash EA® 112 Series (Waltham, Massachusetts, United States) was used to perform sulfur elemental analysis. Sample combustion (1.5 mg) was performed for 15 s at a high temperature (1000 °C) under an oxidizing atmosphere and in the presence of tungstic anhydride. Produced gaseous products (H_2O, SO_2, CO_2, and NOx) were reduced to N_2 in the presence of copper; then, they were analyzed via gas chromatography. The percentage of sulfur present in the compound was calculated by using Eager 300 software.

2.6. Size Exclusion Chromatography (SEC)

SEC was applied to analyze LMPs fractions for molecular weight distributions and averages. Each lignin sample, initially dissolved in 10 mM NaOH at 5 mg/mL under 24 h

magnetic agitation, was filtered with 0.45 μm PTFE filters. Shimadzu Prominence™ (Nara, Japan) chromatography outfitted with a Shimadzu SPD-20A UV detector (280 and 254 nm), a refractive index detector (RID, Shimadzu RID-20A), and Shodex™ GPC KF-806L (Munich, Germany) and Phenogel™ 00H-0442-K0 (Torrance, California, United States) columns were applied. The separation occurred at 35 °C, with elution using 10 mM NaOH at a flow rate of 0.4 mL/min. The calibration curve was plotted using Aligent Technologies® GPC/SEC calibration kits (Aligent PL2090-0101, Santa Clara, California, United States) and the Steinmetz et al. [73] method.

2.7. Nuclear Magnetic Resonance (NMR)

The examination of the lignin structure involved both heteronuclear single quantum coherence (HSQC) and ^{31}P NMR. In a concise procedure for HSQC, 100 mg of purified and dried LMPs was dissolved in 700 μL of dimethyl sulfoxide-d6 (DMSO-d6 99.8%). Spectra were acquired using the Bruker® Avance III 400 MHz spectrometer (Billerica, Massachusetts, United States) at 50 °C with a relaxation delay of 1.5 s. For ^{31}P NMR, the hydroxyl group's content was determined following the published methodology [74], where 25 mg of purified LMPs was dissolved in 400 μL of pyridine/deuterated chloroform (1.6/1 *v*/*v*). A mixed solution (A) of chromium (III) acetylacetonate 97% (3.6 mg/mL) and cyclohexanol (4.0 mg/mL of A) served as the relaxation reagent and internal standard. The solution was derivatized with 50 μL of 2-chloro-4,4,5,5-tetramethyl-1,3,2-dioxaphospholane (TMDP), vortexed, and analyzed using the Bruker® Avance III HD 300 MHz spectrometer at 25 °C with a 25 s relaxation delay. NMR data were processed using Topspin® 4.1.0 software (Bruker Bio Spin, Billerica, Massachusetts, United States).

2.8. Dynamic Light Scattering (DLS)

The Malvern™ Zetasizer ULTRA instrument (Grovewood, United Kingdom) was used to determine the size distribution, size average, polydispersity index (PDI), and ζ-potential of the prepared LNPs suspensions. LNPs suspensions were analyzed immediately after precipitation at 25 °C via complete optical PS cells with a volume of 1.5 mL. Triplicate measurements were recorded in the DLS mode at an angle of 174°. ζ-potential analyses were performed using the same instrument, employing special folded capillary Zeta cells (DTS 1070) at 25 °C.

2.9. Transmission Electron Microscopy (TEM)

LNPs images were captured through an FEI Philips® CM200 transmission electron microscope (TEM, Amsterdam, Netherlands), operating at an accelerating voltage of 160 kV. The samples were directly prepared by applying a drop of LNPs suspension (3 mg/mL) without contrasting agents onto a TEM grid and dried for 30 min.

2.10. Lignin-Based Sunscreen Preparation and Study

As in previous studies [19,27,75], the preparation of sunscreens and the associated SPF measurements were conducted as follows: Each lignin-based sunscreen formulation was generated by mixing LMPs or LNPs powder with corresponding sunscreen or pure cream at 1, 5, and 10 wt% using an IKA® magnetic stirrer at 400 rpm for 14 h in a dark room. After blending, 37.5 mg of lignin-based sunscreen was applied onto a clean 7.5 × 2.5 cm quartz plate of 2 mm thickness to comply with the International sun protection factor (SPF) test method conditions of 2.0 mg/cm^2. The sunscreen was carefully spread across the entire surface by gently rubbing the slide with a nitrile finger cot. Subsequently, the sample was left to dry for 15 min in a dark room before UV transmittance measurements. The UV transmittance of lignin-based sunscreen was measured using a Shimadzu® UV-1900i spectrophotometer. For each lignin-based sunscreen, a minimum of 5 samples were prepared, and measurements were repeated at least 3 times. Transmittance measurements were accumulated in the wavelength spectrum from UVB (290–320 nm) to UVA (320–400

nm). Finally, the *SPF* (Sun protection Factor) value was calculated according to the following equation:

$$SPF = \frac{\sum_{290}^{320} E_\lambda S_\lambda}{\sum_{290}^{320} E_\lambda S_\lambda T_\lambda} \quad (1)$$

where E_λ denotes CIE erythemal efficiency, S_λ denotes solar irradiance, and T_λ denotes the transmittance of the sample. The values of E_λ and S_λ are constants, and they were determined by Sayre et al. [76].

3. Results

The objective of this study was to generate tailored LNPs from various feedstocks through eco-friendly processes and analyze the impact of these parameters on the lignin-based sunscreen's performance.

3.1. LMPs Extraction and Characterization

In order to overcome the current limitations of lignin due to pulping processes, i.e., its extraction using toxic solvents and its relatively high sulfur composition, we purposely used ethanol–organosolv pretreatment without acid catalysis [53]. This method has the advantage of generating clean and pure LMPs with chemical structures that more closely match native lignins compared to kraft ones [53]. The acid-free organosolv process was, therefore, applied to several native biomass types, namely hardwood, softwood, and herbaceous materials. This approach renders it possible to produce lignin fractions with controlled chemical structures, particularly in terms of G, S, and H ratios (Figure 1), which are expected to be crucial for nanometric size reduction and future UV-absorbing properties. The LMPs extraction yields, and physico-chemical features obtained via SEC techniques and NMR (^{31}P, and HSQC) are listed in Table 1. It appears that the organosolv process provides advantages by combining very pure lignin production (93.0%, 96.1%, and 93.3% for beech, spruce, and wheat straw, respectively) with high extraction yields (69.7%, 35.9%, and 44.8% for beech, spruce, and wheat straw, respectively, and based on raw lignin biomass content). In addition, the isolation process leads to sulfur-free lignins, while commercial kraft lignin contains up to 1.8% sulfur, which is a key factor for potential product development.

The LMPs molecular weight (Mw) is presented in Tables 1 and S1. It appears that organosolv delignification treatment led to Mw reduction, which is consistent with lignin breakdown. Furthermore, all three lignin samples extracted using the organosolv process had a lower average Mw (20.8, 15.7, and 17.2 kDa for beech, spruce, and wheat straw, respectively) than the lignin derived from the kraft process (29.4 kDa). These results suggest that both types of feedstock and the extraction process parameters play a part in lignin reaction mechanisms, such as depolymerization and recondensation.

Table 1. LMPs isolation yields and characterization for beech, spruce, wheat straw, and kraft lignin. Mw represents the average molecular weight.

LMPs Characterizations	Organosolv 200 °C 60 min 60/40 EtOH/H_2O (*v*/*v*)			Kraft
	Beech	Spruce	Wheat Straw	
Extraction yields (wt%)	69.7 ± 0.8	35.9 ± 1.2	44.8 ± 0.4	/
Purity (%)	93.0 ± 0.4	96.1 ± 0.1	96.3 ± 0.7	91.5 ± 0.3
Sulfur content (%)	<0.05	<0.05	<0.05	1.8
Mw (kDa)	20.8	15.7	17.2	29.4

LMPs extraction (wt%) yields are based on raw lignin biomass content. Results include lignin purity (%), sulfur content (%), and average Mw from SEC.

In order to further investigate the chemical structure of different recovered LMPs, ^{31}P and two-dimensional HSQC NMR measurements were performed. Table 2 shows the

structural assignments and number (mmol.g^{-1} of lignin) of main ^{31}P NMR signals for phosphitylated LMPs.

Table 2. Physico–chemical analysis of lignin extracts.

^{31}P Nuclear Magnetic Resonance (NMR)—Hydroxyl Groups (mmol.g^{-1})				
LMPs	**Beech**	**Spruce**	**Wheat Straw**	**Kraft**
Total -OH	4.19	3.71	2.94	4.62
Aliphatic -OH	2.26	1.71	1.27	1.68
Phenolic -OH	1.93	1.86	1.44	2.53
Syringyl	1.18	0.14	0.59	0.36
Guaiacyl	0.74	1.59	0.61	2.17
p-Hydroxypenyl	0.01	0.13	0.24	0
COOH	0	0.14	0.23	0.41
Heteronuclear single quantum coherence (HSQC) NMR spectroscopy—linkages (%)				
LMPs	**Beech**	**Spruce**	**Wheat straw**	**Kraft**
β-O-4 (%)	25.28	17.89	16.09	9.65
β-5 (%)	3.94	13.71	3.94	2.44
β-β (%)	6.76	3.06	1.40	3.72
S/G	1.87	0	1.03	0

Considering the former ^{31}P NMR results obtained from milled wood lignin (MWL) reported by Brosse et al. [77] and Qian et al. [74], a significant increase in phenolic -OH groups was observed due to the β-O-4 aryl ether acidolysis. Kraft lignin appears to undergo higher recondensation according to ^{31}P NMR results, with a substantial increase in guaiacyl -OH amounts compared to spruce organosolv lignin. In addition, HSQC NMR analyses were conducted in order to investigate side chains and aromatic region change ratios (β-O-4, β-5, β-β, and S/G amount in %). Milled wood results for the extracted lignin in Table S1 confirmed that organosolv pretreatment led to lignin depolymerization, which was highlighted by β-O-4 acidolytic breakdown. The elevated S/G ratios observed in both beech and wheat straw also indicate lignin depolymerization. Regarding comparative results obtained with organosolv spruce lignin isolation versus kraft lignin, the findings indicate that the kraft process has a more severe influence on chemical structure by promoting depolymerization and recondensation.

It can be concluded that, independently of the feedstock source, organosolv allows the extraction of a lignin type that is close to the native one, with less depolymerization and recondensation compared with the kraft process. Moreover, in accordance with the studies of Adamcyk et al. [53] and Siika-aho et al. [78], delignification and lignin depolymerization are easier for both hardwood and herbaceous materials compared to softwood with respect to the same process severities. Nevertheless, herbaceous material processing challenges still need to be addressed due to their low density and important ash content compared to hardwood and softwood biomass, which makes it necessary to implement specific optimizations for efficient fractionation steps.

3.2. LNPs Production and Characterization

The size distribution, average size, and ζ-potential of LNPs suspensions obtained according to the manufacturing process described above were analyzed using a Malvern™ Zetasizer, as shown in Figure 2. Nanosized, monomodal, and size distributions that are quite large were observed in all cases. The mean size of the particles calculated in terms of scattered intensity decreases in the order kraft > wheat straw > spruce > beech lignin. The mean sizes of particles obtained from beech, spruce, and wheat straw are similar, while particles obtained from kraft lignin are much larger (mean size of 198 nm). The results in Figure 2 support the theory that LNPs formation mechanisms are partly driven by

lignin chemical structure interactions [62,79–81] since the chemical compositions of lignin molecules extracted from beech, spruce, and wheat straw have more similarities between them than kraft. This highlights the crucial importance of selecting the appropriate biomass for further processing and application. However, the distribution and mean particle size of beech, spruce, and wheat straw do not fall below the limit value of 45 nm defined by Filon et al. [55] with respect to potential skin penetration, providing no restrictions for cosmetic applications. Figure 2 also shows the ζ-potential of the LNPs suspensions. The results revealed a highly negative ζ-potential with respect to all suspensions (−26 to −33 mV), which favors maintaining self-repulsion and electrostatic stability over time. This is confirmed by the very low variation of the particle mean sizes after 90 days of storage at 4 °C (size variation between 3 and 10%).

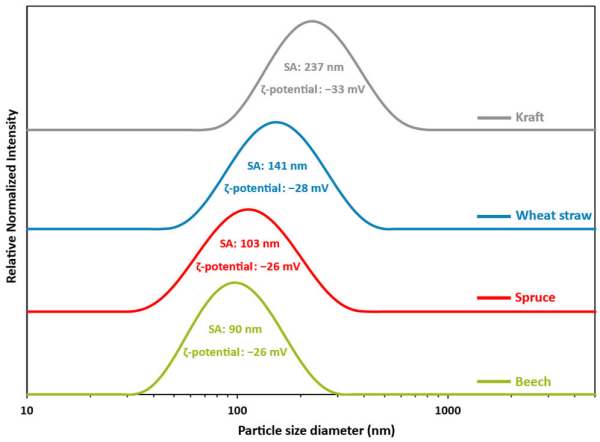

Figure 2. LNPs particles size distributions obtained from a pool of 3 batches, each prepared according to the described protocol: LMPs concentration: 30 mg/mL. Addition rate: 100 mL/min. Anti-solvent composition: 100% water. Dilution ratio: 1/10. T °C: 20 °C. Stirring speed: 500 rpm. SA: size average. PI: polydispersity index. Green: beech; PI = 0.148. Red: spruce; PI = 0.183. Blue: wheat straw; PI = 0.185. Grey: kraft; PI = 0.193.

TEM microscopic observations in Figure 3 were used to complete the characterization of LNPs. First, TEM images confirm the DLS measurements for each lignin source. Nevertheless, while particles from beech feedstock appeared to be spherical and isotropic, particles from other feedstocks seem to present irregular shapes, as well as anisotropy characterized by a dense core enveloped in a fluffy outer wreath. Finally, it can be observed that Kraft lignin has the most irregular shape and the highest anisotropy.

The multiparameter mechanism behind the formation of lignin nanoparticles in the anti-solvent system can be partially explained by considering the well-documented amphiphilic nature of lignin polymers, as extensively carried out in the literature [61,80–82]. Higher phenolic hydroxyl and carboxyl contents enhanced hydrophilicity, while non-covalent π–π interactions contribute to hydrophobicity, especially in lignin with more S units (S > G > H). Consequently, hydrophobic lignin solutions guided by π–π stacking and the S/G ratio yield smaller and more spherical LNPs [83]. Conversely, hydrophilic solutions containing lignins extracted from kraft result in the formation of larger and more irregular nanoparticles due to the presence of hydrophilic components that twist towards the surface of the particle during its formation, thus perturbating the self-assembling process and consequently the aggregation phenomenon (Table 2, Figures 2 and 3) [79].

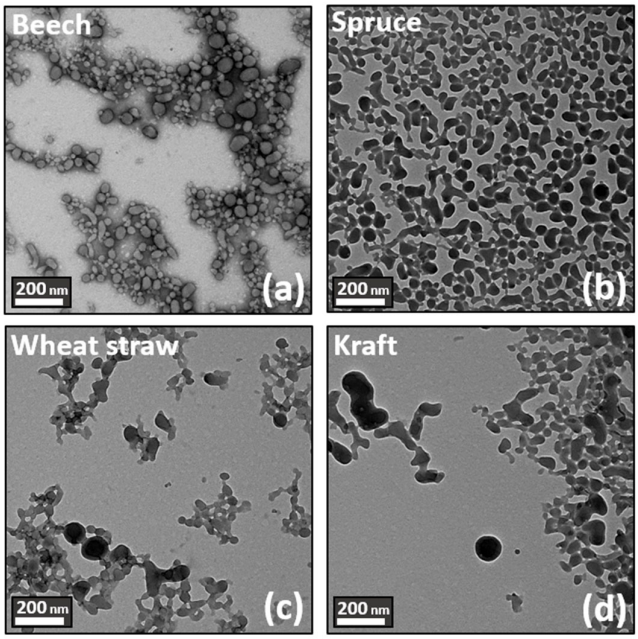

Figure 3. TEM images of the suspension generated according to the fractionation process and biomass source. Top left: (**a**) beech. Top right: (**b**) spruce. Bottom left: (**c**) wheat straw. Bottom right: (**d**) kraft.

It can, therefore, be concluded that an optimized LNPs manufacturing method was designed. This procedure allows the obtainment of high production yields and well-defined particle properties (size, shape, stability, and polydispersity) without strongly and negatively impacting the environment from the formulation stage. This is a strong innovative step since, up until now, lignin size reduction had been widely implemented during precipitation with respect to hazardous, toxic, or explosive solvents such as tetrahydrofuran (THF), pyridine, or dimethyl sulfoxide (DMSO) [27].

3.3. Lignin-Based Sunscreen Analysis

For this part, diverse lignin-based sunscreen samples were prepared following the outlined procedure. The investigations focused on assessing the impact of various parameters on UV-absorption sunscreen efficacy, including particle concentration, lignin chemical structure (feedstock and isolation process), and particle size. In each formulation, lignin particles were directly mixed into commercial creams with varying sun protection factors (SPF 1, SPF 10, and SPF 30) to assess the UV-shielding ability of lignin, both with and without other commercial filters. The results were also compared with pure SPF 10 and SPF 30 commercial sunscreens as references. The transmittance and related SPF values of lignin-based sunscreen were measured in the UVA (320–400 nm) and UVB (290–320 nm) ranges, with the results summarized in the following section. First, Figure 4 and Table 3 results indicated that the pure cream (NIVEA® Soft) was UV-filter-free, with a maximum transmittance of 95–90%, corresponding to an SPF of 1.08.

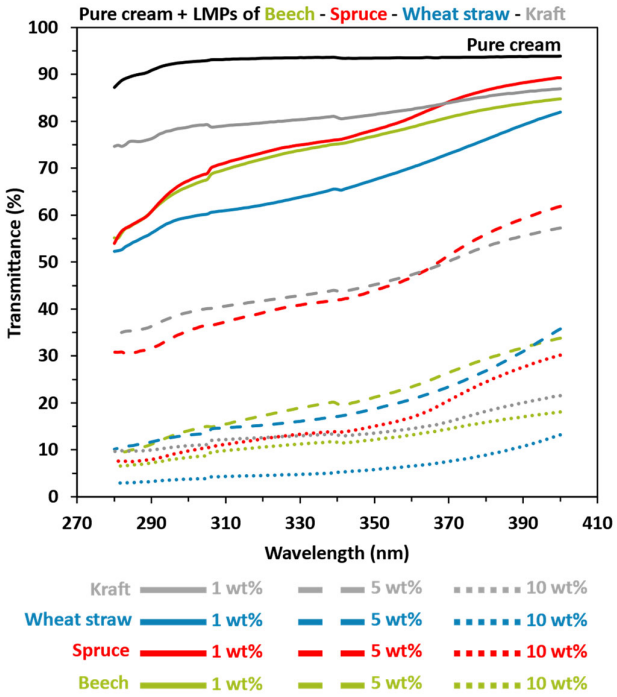

Figure 4. UV transmittance results in the UVA and UVB area of pure cream (NIVEA® Soft) mixed with 1, 5, or 10 wt% lignin macroparticles (LMPs). Black: pure cream. Green: beech. Red: spruce. Blue: wheat straw. Grey: kraft. Solid lines: 1 LMPs wt%. Coarse dotted lines: LMPs 5 wt%. Fine dotted line: LMPs 10 wt%.

Table 3. Measured SPF values for lignin-based pure cream and commercial sunscreens.

LMPs (wt%)	**0** [a]	**Beech**			**Spruce**			**Wheat Straw**			**Kraft**		
		1	**5**	**10**	**1**	**5**	**10**	**1**	**5**	**10**	**1**	**5**	**10**
Pure cream	1.08 ± 0.02	1.48 ± 0.03	6.77 ± 1.09	11.24 ± 0.24	1.45 ± 0.05	2.76 ± 0.13	9.65 ± 1.23	1.66 ± 0.02	7.33 ± 1.37	25.30 ± 4.31	1.27 ± 0.02	2.51 ± 0.65	8.85 ± 1.21
LMPs (wt%)	**0** [b]	**1**		**5**	**1**		**5**	**1**		**5**	**1**		**5**
*** SPF 10**	9.39 ± 0.53	27.43		50+	13.70		26.17	18.29		50+	11.88		22.65
LMPs (wt%)	**0** [c]	**1**			**1**			**1**			**1**		
*** SPF 30**	30.93 ± 4.97	50+			50+			50+			50+		
LNPs (wt%)	**0** [a]	**Beech**			**Spruce**			**Wheat straw**					
		1		**5**	**1**		**5**	**1**		**5**			
Pure cream	1.08 ± 0.02	4.93 ± 0.53		20.17 ± 2.20	3.41 ± 0.96		11.39 ± 1.32	7.88 ± 0.84		41.97 ± 7.38			

[a] Commercial pure cream without UV-shielding properties. [b] Commercial sunscreen with SPF 10 without lignin addition. [c] Commercial sunscreen with SPF 30 and without lignin addition. * Commercial sunscreens.

Then, Figure 4 confirms the former results from the literature [19,20,22,24,26,28,75], with a decrease in UV transmittance linked to an increase in SPF values when LMPs were added to pure cream, regardless of the lignin type or biomass feedstock. The SPF values of the 1 wt% LMPs-based pure cream ranged from 1.27 to 1.66, with lower transmittance in both UVA and UVB areas for organosolv–wheat straw lignin (OWS). A substantial gap was observed with respect to 5 wt% of LMPs concerning kraft and organosolv–spruce

(OS) compared to organosolv–beech (OB) and wheat straw lignins (SPF values from 2.51 and 7.33). Indeed, the results from 5 wt% LMPs-based OWS and OB pure cream were practically equivalent to kraft and OS 10 wt%. For the 10 wt% amount, OWS stands out from other preparations with an SPF of 25.30 compared to 11.24, 9.65, and 8.85 for OB, OS, and kraft lignin, respectively.

Close trends were therefore observed for hardwood and herbaceous species: transmittance decreases related to UV shielding follow the lignin concentration of lignin-based cream. Conversely, for softwood species, the UV-shielding evolution is more gradational depending on the total amount of lignin inside the cream. The improved results compared to the literature [19,20,22,26] can be explained by the use of organosolv lignin demonstrated by Qian et al. [20], which is most suitable for high-SPF cream. It is also explained by effective homogeneity (i.e., distribution of LMPs in pure cream or commercial sunscreen without aggregates, Figure S1), even with macrolignin compared to the Zhang et al. [75] work.

Currently, if the brown characteristic color of lignin is still a problem, the solution may lie in the use of this natural organic filter as a complement to current filters in order to reduce their proportions. Therefore, the enhancement of commercial SPF 10 and SPF 30 sunscreens with LMPs was also studied. Results in Figures 5 and S2 indicate that LMPs improve both commercial SPF 10 and SPF 30 sunscreens. The same trends were observed, with hardwood and herbaceous LMPs exhibiting better UV-shielding properties with the transmittance of SPF 10 + 1 wt%, closely matching commercial SPF 30 sunscreens (SPF values of 18.29 and 27.43). For softwood LMPs, even at 5 wt% concentration, the transmittance of SPF 10 corresponds to the SPF 30 sunscreen (SPF values of 22.65 and 26.17). In the case of adding 1 wt% of LMPs in the commercial SPF 30 lotion, the total UV-shielding transmittance value was close to 0 and exhibited highly related SPF values (SPF > 100, but it was indexed at 50+ for a concrete meaning).

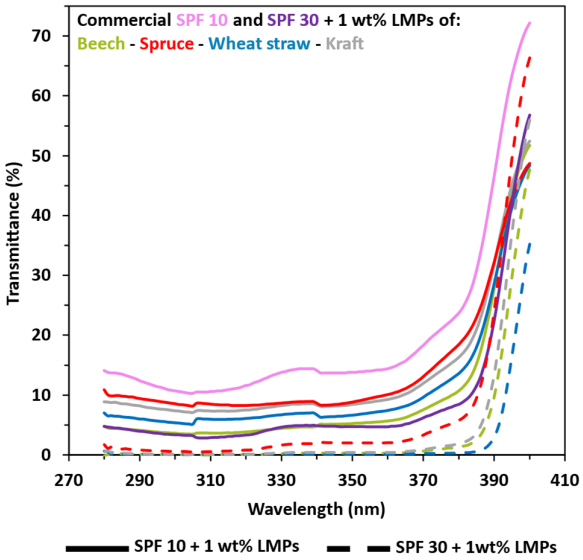

Figure 5. UV transmittance results in UVA and UVB areas from 1 wt% lignin macroparticles (LMPs) blended with SPF 10 (pink) and SPF 30 (purple) commercial sunscreen. Green: beech. Red: spruce. Blue: wheat straw. Grey: kraft. Solid line: commercial SPF 10 sunscreen + LMPs. Coarse dotted line: commercial SPF 30 sunscreen + LMPs. Other results are available in ESI.

The enhanced properties observed in a cream blended with lignin can be attributed to two potential factors. First, the chemical composition of the UV filter and its interactions with the constituents of the cream play a crucial role, as was previously demonstrated. Additionally, the size and geometry of the adding filter also contribute to these

improvements. Consequently, as shown in Figure 6, we prepared LNPs-based (NIVEA® Soft) on 1 wt% and 5 wt% pure cream from OB, OS, and OWS lignins in order to quantify the reduction size impact over the pure cream properties (UV-shielding and color). Once again, increasing the amount of lignin improved the blended pure cream (NIVEA® Soft) properties, with the following advantage: herbaceous > hardwood > softwood. Indeed, SPF results for the 1 wt% LNP-based pure cream were 7.88, 4.93, and 3.41 for wheat straw, beech, and spruce, respectively. When the creams were prepared with 5 wt% of LNPs, the SPF reached values of 41.97, 20.17, and 11.39 for the same extracted lignin samples.

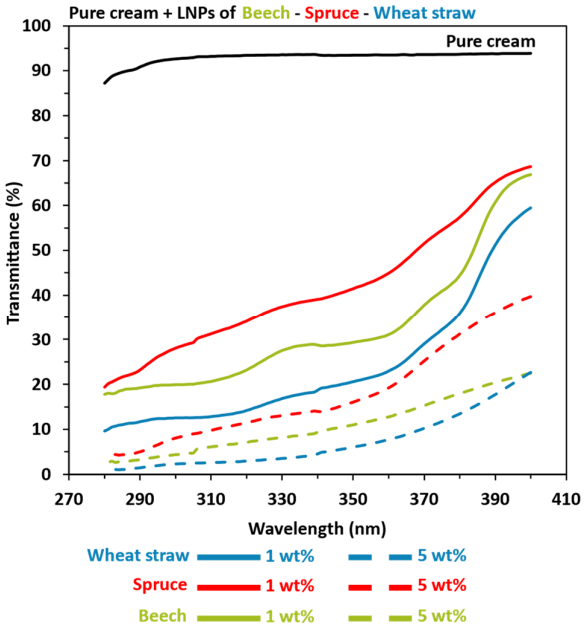

Figure 6. UV transmittance results in UVA and UVB areas of pure cream (NIVEA® Soft) mixed with 1 or 5 wt% lignin nanoparticles (LNPs). Black: pure cream. Green: beech. Red: spruce. Blue: wheat straw. Solid line: 1 LNPs wt%. Coarse dotted line: 5 wt% LNPs.

By comparing UV-shielding properties between prepared LMPs and LNPs pure creams in Figure 7, the lignin particle size impact was demonstrated. Indeed, macro- to nanoscale reductions improved the UVB average transmittance of pure creams prepared with the same lignin wt% from 2.5 to 6.5. Thus, close UVB average transmittance values were not only observed between LMPs 5 wt% and LNPs 1 wt% but also between LMPs 10 wt% and LNPs 5 wt%, which consequently revealed a correspondent brown color reduction for LNPs-based pure cream (Figure S1). Ultimately, sunscreens incorporating 5 wt% LNPs derived from the organosolv extraction achieved SPF values of 20.17, 11.39, and 41.97 for beech, spruce, and wheat straw, respectively, closely approximating those of high-protection lotions with minimal organic UV filter content (Table 3).

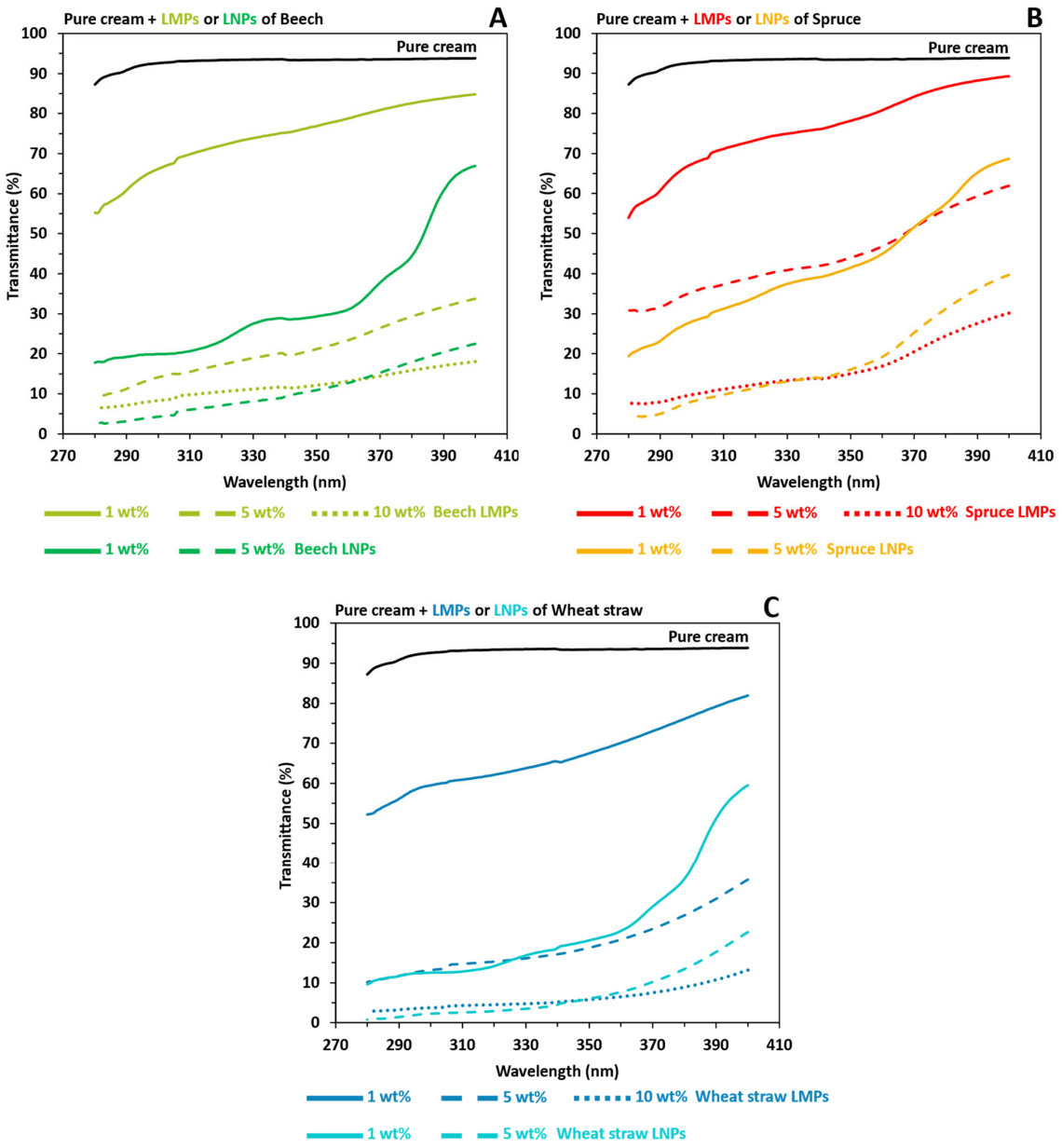

Figure 7. UV transmittance results in the UVA and UVB areas of pure cream (NIVEA® Soft) mixed with the macroparticles (LMPs) or nanoparticles (LNPs) of extracted organosolv lignins. Black: pure cream. (**A**) Beech LMPs or LNPs. Light green: LMPs. Dark green: LNPs. (**B**) Spruce LMPs or LNPs. Red: LMPs. Orange: LNPs. (**C**) Wheat straw LMPs or LNPs. Dark blue: LMPs. Light blue: LNPs. For (**A**–**C**), solid line: 1 LNPs wt%. Coarse dotted line: 5 wt% LNPs.

3.4. Factors Affecting Lignin UV-Shielding Properties

It is generally accepted that there are several factors affecting the UV-blocking performances of lignin polymers. These factors manifest in two different forms according to Zhang et al. [84]: (1) the intrinsic chemical structure of lignin relies on the biomass nature, and (2) the extrinsic factors, including the size, shape, and purity of lignin particles, are determined via extraction and nanoparticle fabrication processes:

(1) Lignin UV-shielding properties are related to chromophore functional groups and especially phenolic hydroxyl groups [22,27,31,75,84]. Guo et al. [85] previously demonstrated that the S phenolic group exhibited stronger UV-absorbing properties

due to the additional methoxyl group compared to the G and H units (Figure 1). Consequently, this enhanced the abundance of free electron pairs from oxygen atoms. Part of the results aligns with these explanations, such as beech and wheat straw biomass, which present advantageous chemical structures (high S/G phenolic hydroxyl content, i.e., high methoxy content and darker [24] color) and had greater UV-shielding properties compared to spruce lignin. It was previously demonstrated by Wang et al. [26] that the lignin chemical structure remains unchanged with respect to the nanoprecipitation process, which explains why the same trends can be observed between sunscreens prepared with both LMPs and LNPs. However, the observation that wheat straw lignin exhibited superior, stronger UV-shielding properties over beech lignin suggests that while methoxyl groups and phenolic units may be predominant, they do not fully account for all aspects of lignin-enhanced UV protection. The complex and interconnected structure of wheat straw lignin with proven tricin units [71] and other phenolic end groups, such as aryl acetic acid, can also contribute to the enhanced UV-shielding properties observed in herbaceous lignins [86]. Other chromophores in lignin, such as quinones or -CH=CH-, -C=C-, and -C=O bonds [84] and M_w [87], can contribute to UVB and UVA absorbance.

(2) Although the extrinsic properties of lignin are often given less consideration, particle size, shape, and purity can be modified by processes and are also important factors that can explain UV absorption properties. First, the relatively highest level of impurities (7%) was found in beech lignin compared to other organosolv-extracted lignin (3.7 and 3.9% for wheat straw and spruce, respectively), which may reduce UV-shielding properties to a greater extent. In the case of kraft, 9.5% of the impurities coupled with 1.8% sulfur presence can also contribute to lower UV absorption despite a large number of aromatic rings. Regarding lignin particle size and morphology, recent studies [22,88] showed that lignin nanoparticles compared to macroparticles have a higher specific surface area, higher transparency, better dispersibility, and, consequently, better UV-shielding properties per weight (Figure S1). Reduced particle size induces a higher specific surface area, thereby permitting the greater availability of chromophores per unit weight. This results in enhanced UV-shielding properties, lighter coloration, and improved dispersion within the sunscreen formulation and ultimately leads to a reduced reliance on organic UV filter (Figure S1). The results from this study have indeed proven previous observations with respect to a general decrease in UVB average transmittance between 2.5 and 6.5 with the same lignin types but different size scales. With respect to particle shape, Tan et al. [70] showed that the spherical (better A/V ratio) design provided a larger surface area because of the minimum packing density compared with other forms, thus allowing higher chromophore availability and concentration, which can boost UV absorption properties.

4. Conclusions

Various sunscreen formulations incorporating the macro- and nanoparticles of lignin biopolymers as a natural UV filter were successfully produced in an ecological and simple manner from different biomass by-products and isolation processes. Consequently, the importance of lignin's intrinsic (chemical structure) and extrinsic parameters (lignin extraction and LNPs properties) over the UV-shielding properties of sunscreens was highlighted and quantified. First, with respect to chemical structures, grass and hardwoods exhibit a higher prevalence of methoxy groups, resulting in a 2.5 times performance improvement compared to softwoods regardless of particle size and concentration. Then, reducing the particle size from the macro- to nanoscale enhances dispersion, increases specific surface area, and, consequently, amplifies UV absorbance, resulting in a color reduction and improvements between 2.5- and 6.5-fold, irrespective of the lignin's nature and concentration. From this observation, sunscreen formulated with 5 wt% LNPs from wheat straw achieved an SPF value of 41.97, approaching that of high-protection lotions.

When added to commercial sunscreens, lignin boosted performances, while reducing synthetic filter concentrations, providing 50+ protection from SPF 10 lotion with 5 wt% of LMPs. This study provides a simple approach for lignin polymer valorization with the formulation of sunscreens using eco-friendly LNPs.

Supplementary Materials: The following supporting information can be downloaded at https://www.mdpi.com/article/10.3390/polym16131901/s1. Table S1: Milled wood lignin (MWL) molecular weights and main lignin linkages (%).a Results for untreated wheat straw lignin from Auxenfans et al. [89].; Figure S1: Appearance of each produced sunscreen; Figure S2: UV transmittance of commercial SPF 10 sunscreen mixed with 5 wt% LMPs from organosolv (beech, spruce, and wheat straw) or kraft (spruce) processes in UVA and UVB areas.

Author Contributions: V.G.: Conceptualization, analysis, investigation, and writing—original draft. L.F.: Investigation. H.C.: Project administration, supervision, and investigation. N.B.: Writing—review and editing. L.M.-H.: Investigation, methodology, and analysis. N.C.: Investigation, methodology, and analysis. S.P.: Resources and validation. I.Z.-D.: Project administration, funding acquisition, supervision, methodology, investigation, and analysis. All authors have read and agreed to the published version of the manuscript.

Funding: The authors thank the French National Research Agency and the Grand Est Region for their financial support provided through the ARBRE Laboratory of Excellence (ARBRE; grant ANR-11-LABX-0002-01).

Institutional Review Board Statement: Not applicable.

Data Availability Statement: The original contributions presented in the study are included in the article/supplementary material, further inquiries can be directed to the corresponding author/s.

Acknowledgments: The authors also express their deep appreciation with respect to the Plateforme PhotoNS of the L2CM Laboratory, University of Lorraine, and the CC3M of the IJL Laboratory, University of Lorraine.

Conflicts of Interest: The authors declare no conflicts of interest.

References

1. Diaz, J.H.; Nesbitt, L.T. Sun Exposure Behavior and Protection: Recommendations for Travelers. *J. Travel Med.* **2013**, *20*, 108–118. https://doi.org/10.1111/j.1708-8305.2012.00667.x.
2. Young, A.R.; Narbutt, J.; Harrison, G.I.; Lawrence, K.P.; Bell, M.; O'Connor, C.; Olsen, P.; Grys, K.; Baczynska, K.A.; Rogowski-Tylman, M.; et al. Optimal Sunscreen Use, during a Sun Holiday with a Very High Ultraviolet Index, Allows Vitamin D Synthesis without Sunburn. *Br. J. Dermatol.* **2019**, *181*, 1052–1062. https://doi.org/10.1111/bjd.17888.
3. Gilbert, E.; Pirot, F.; Bertholle, V.; Roussel, L.; Falson, F.; Padois, K. Commonly Used UV Filter Toxicity on Biological Functions: Review of Last Decade Studies. *Int. J. Cosmet. Sci.* **2013**, *35*, 208–219. https://doi.org/10.1111/ics.12030.
4. Schneider, S.L.; Lim, H.W. A Review of Inorganic UV Filters Zinc Oxide and Titanium Dioxide. *Photodermatol. Photoimmunol. Photomed.* **2019**, *35*, 442–446. https://doi.org/10.1111/phpp.12439.
5. Giokas, D.L.; Salvador, A.; Chisvert, A. UV Filters: From Sunscreens to Human Body and the Environment. *TrAC Trends Anal. Chem.* **2007**, *26*, 360–374. https://doi.org/10.1016/j.trac.2007.02.012.
6. Damiani, E.; Astolfi, P.; Giesinger, J.; Ehlis, T.; Herzog, B.; Greci, L.; Baschong, W. Assessment of the Photo-Degradation of UV-Filters and Radical-Induced Peroxidation in Cosmetic Sunscreen Formulations. *Free Radic. Res.* **2010**, *44*, 304–312. https://doi.org/10.3109/10715760903486065.
7. Levine, A. Sunscreen Use and Awareness of Chemical Toxicity among Beach Goers in Hawaii Prior to a Ban on the Sale of Sunscreens Containing Ingredients Found to Be Toxic to Coral Reef Ecosystems. *Mar. Policy* **2020**, *117*, 103875. https://doi.org/10.1016/j.marpol.2020.103875.
8. Downs, C.A.; Kramarsky-Winter, E.; Fauth, J.E.; Segal, R.; Bronstein, O.; Jeger, R.; Lichtenfeld, Y.; Woodley, C.M.; Pennington, P.; Kushmaro, A.; et al. Toxicological Effects of the Sunscreen UV Filter, Benzophenone-2, on Planulae and in Vitro Cells of the Coral, Stylophora Pistillata. *Ecotoxicology* **2014**, *23*, 175–191. https://doi.org/10.1007/s10646-013-1161-y.
9. Corinaldesi, C.; Marcellini, F.; Nepote, E.; Damiani, E.; Danovaro, R. Impact of Inorganic UV Filters Contained in Sunscreen Products on Tropical Stony Corals (Acropora Spp.). *Sci. Total Environ.* **2018**, *637–638*, 1279–1285. https://doi.org/10.1016/j.scitotenv.2018.05.108.
10. Ouchene, L.; Litvinov, I.V.; Netchiporouk, E. Hawaii and Other Jurisdictions Ban Oxybenzone or Octinoxate Sunscreens Based on the Confirmed Adverse Environmental Effects of Sunscreen Ingredients on Aquatic Environments. *J. Cutan. Med. Surg.* **2019**, *23*, 648–649. https://doi.org/10.1177/1203475419871592.

11. Adler, B.L.; DeLeo, V.A. Sunscreen Safety: A Review of Recent Studies on Humans and the Environment. *Curr Derm Rep* **2020**, *9*, 1–9. https://doi.org/10.1007/s13671-020-00284-4.
12. Widsten, P. Lignin-Based Sunscreens—State-of-the-Art, Prospects and Challenges. *Cosmetics* **2020**, *7*, 85. https://doi.org/10.3390/cosmetics7040085.
13. Tan, S.S.Y.; MacFarlane, D.R.; Upfal, J.; Edye, L.A.; Doherty, W.O.S.; Patti, A.F.; Pringle, J.M.; Scott, J.L. Extraction of Lignin from Lignocellulose at Atmospheric Pressure Using Alkylbenzenesulfonate Ionic Liquid. *Green Chem.* **2009**, *11*, 339. https://doi.org/10.1039/b815310h.
14. Wei, Z.; Yang, Y.; Yang, R.; Wang, C. Alkaline Lignin Extracted from Furfural Residues for pH-Responsive Pickering Emulsions and Their Recyclable Polymerization. *Green Chem.* **2012**, *14*, 3230. https://doi.org/10.1039/c2gc36278c.
15. Thakur, V.K.; Thakur, M.K.; Raghavan, P.; Kessler, M.R. Progress in Green Polymer Composites from Lignin for Multifunctional Applications: A Review. *ACS Sustain. Chem. Eng.* **2014**, *2*, 1072–1092. https://doi.org/10.1021/sc500087z.
16. Ragauskas, A.J.; Beckham, G.T.; Biddy, M.J.; Chandra, R.; Chen, F.; Davis, M.F.; Davison, B.H.; Dixon, R.A.; Gilna, P.; Keller, M.; et al. Lignin Valorization: Improving Lignin Processing in the Biorefinery. *Science* **2014**, *344*, 1246843. https://doi.org/10.1126/science.1246843.
17. Calvo-Flores, F.G.; Dobado, J.A. Lignin as Renewable Raw Material. *ChemSusChem* **2010**, *3*, 1227–1235.
18. Bajwa, D.S.; Pourhashem, G.; Ullah, A.H.; Bajwa, S.G. A Concise Review of Current Lignin Production, Applications, Products and Their Environmental Impact. *Ind. Crops Prod.* **2019**, *139*, 111526. https://doi.org/10.1016/j.indcrop.2019.111526.
19. Qian, Y.; Qiu, X.; Zhu, S. Lignin: A Nature-Inspired Sun Blocker for Broad-Spectrum Sunscreens. *Green Chem.* **2015**, *17*, 320–324. https://doi.org/10.1039/C4GC01333F.
20. Qian, Y.; Qiu, X.; Zhu, S. Sunscreen Performance of Lignin from Different Technical Resources and Their General Synergistic Effect with Synthetic Sunscreens. *ACS Sustain. Chem. Eng.* **2016**, *4*, 4029–4035. https://doi.org/10.1021/acssuschemeng.6b00934.
21. Wang, J.; Deng, Y.; Qian, Y.; Qiu, X.; Ren, Y.; Yang, D. Reduction of Lignin Color via One-Step UV Irradiation. *Green Chem.* **2016**, *18*, 695–699. https://doi.org/10.1039/C5GC02180D.
22. Qian, Y.; Zhong, X.; Li, Y.; Qiu, X. Fabrication of Uniform Lignin Colloidal Spheres for Developing Natural Broad-Spectrum Sunscreens with High Sun Protection Factor. *Ind. Crops Prod.* **2017**, *101*, 54–60. https://doi.org/10.1016/j.indcrop.2017.03.001.
23. Gordobil, O.; Herrera, R.; Yahyaoui, M.; İlk, S.; Kaya, M.; Labidi, J. Potential Use of Kraft and Organosolv Lignins as a Natural Additive for Healthcare Products. *RSC Adv.* **2018**, *8*, 24525–24533. https://doi.org/10.1039/C8RA02255K.
24. Lee, S.C.; Tran, T.M.T.; Choi, J.W.; Won, K. Lignin for White Natural Sunscreens. *International Journal of Biological Macromolecules* **2019**, *122*, 549–554. https://doi.org/10.1016/j.ijbiomac.2018.10.184.
25. Lee, S.C.; Yoo, E.; Lee, S.H.; Won, K. Preparation and Application of Light-Colored Lignin Nanoparticles for Broad-Spectrum Sunscreens. *Polymers* **2020**, *12*, 699. https://doi.org/10.3390/polym12030699.
26. Wang, B.; Sun, D.; Wang, H.-M.; Yuan, T.-Q.; Sun, R.-C. Green and Facile Preparation of Regular Lignin Nanoparticles with High Yield and Their Natural Broad-Spectrum Sunscreens. *ACS Sustain. Chem. Eng.* **2019**, *7*, 2658–2666. https://doi.org/10.1021/acssuschemeng.8b05735.
27. Zhang, H.; Liu, X.; Fu, S.; Chen, Y. Fabrication of Light-Colored Lignin Microspheres for Developing Natural Sunscreens with Favorable UV Absorbability and Staining Resistance. *Ind. Eng. Chem. Res.* **2019**, *58*, 13858–13867. https://doi.org/10.1021/acs.iecr.9b02086.
28. Zhang, H.; Liu, X.; Fu, S.; Chen, Y. High-Value Utilization of Kraft Lignin: Color Reduction and Evaluation as Sunscreen Ingredient. *Int. J. Biol. Macromol.* **2019**, *133*, 86–92. https://doi.org/10.1016/j.ijbiomac.2019.04.092.
29. Trevisan, H.; Rezende, C.A. Pure, Stable and Highly Antioxidant Lignin Nanoparticles from Elephant Grass. *Ind. Crops Prod.* **2020**, *145*, 112105. https://doi.org/10.1016/j.indcrop.2020.112105.
30. Ratanasumarn, N.; Chitprasert, P. Cosmetic Potential of Lignin Extracts from Alkaline-Treated Sugarcane Bagasse: Optimization of Extraction Conditions Using Response Surface Methodology. *Int. J. Biol. Macromol.* **2020**, *153*, 138–145. https://doi.org/10.1016/j.ijbiomac.2020.02.328.
31. Widsten, P.; Tamminen, T.; Liitiä, T. Natural Sunscreens Based on Nanoparticles of Modified Kraft Lignin (CatLignin). *ACS Omega* **2020**, *5*, 13438–13446. https://doi.org/10.1021/acsomega.0c01742.
32. Ugartondo, V.; Mitjans, M.; Vinardell, M. Comparative Antioxidant and Cytotoxic Effects of Lignins from Different Sources. *Bioresour. Technol.* **2008**, *99*, 6683–6687. https://doi.org/10.1016/j.biortech.2007.11.038.
33. Tortora, M.; Cavalieri, F.; Mosesso, P.; Ciaffardini, F.; Melone, F.; Crestini, C. Ultrasound Driven Assembly of Lignin into Microcapsules for Storage and Delivery of Hydrophobic Molecules. *Biomacromolecules* **2014**, *15*, 1634–1643. https://doi.org/10.1021/bm500015j.
34. Gil-Chávez, G.J.; Padhi, S.S.P.; Pereira, C.V.; Guerreiro, J.N.; Matias, A.A.; Smirnova, I. Cytotoxicity and Biological Capacity of Sulfur-Free Lignins Obtained in Novel Biorefining Process. *Int. J. Biol. Macromol.* **2019**, *136*, 697–703. https://doi.org/10.1016/j.ijbiomac.2019.06.021.
35. Gordobil, O.; Oberemko, A.; Saulis, G.; Baublys, V.; Labidi, J. In Vitro Cytotoxicity Studies of Industrial Eucalyptus Kraft Lignins on Mouse Hepatoma, Melanoma and Chinese Hamster Ovary Cells. *Int. J. Biol. Macromol.* **2019**, *135*, 353–361. https://doi.org/10.1016/j.ijbiomac.2019.05.111.
36. Freitas, F.M.C.; Cerqueira, M.A.; Gonçalves, C.; Azinheiro, S.; Garrido-Maestu, A.; Vicente, A.A.; Pastrana, L.M.; Teixeira, J.A.; Michelin, M. Green Synthesis of Lignin Nano- and Micro-Particles: Physicochemical Characterization, Bioactive Properties and Cytotoxicity Assessment. *Int. J. Biol. Macromol.* **2020**, *163*, 1798–1809. https://doi.org/10.1016/j.ijbiomac.2020.09.110.

37. Menima-Medzogo, J.A.; Walz, K.; Lauer, J.C.; Sivasankarapillai, G.; Gleuwitz, F.R.; Rolauffs, B.; Laborie, M.-P.; Hart, M.L. Characterization and In Vitro Cytotoxicity Safety Screening of Fractionated Organosolv Lignin on Diverse Primary Human Cell Types Commonly Used in Tissue Engineering. *Biology* **2022**, *11*, 696. https://doi.org/10.3390/biology11050696.
38. Ralph, J.; Lundquist, K.; Brunow, G.; Lu, F.; Kim, H.; Schatz, P.F.; Marita, J.M.; Hatfield, R.D.; Ralph, S.A.; Christensen, J.H.; et al. Lignins: Natural Polymers from Oxidative Coupling of 4-Hydroxyphenyl-Propanoids. *Phytochem. Rev.* **2004**, *3*, 29–60. https://doi.org/10.1023/B:PHYT.0000047809.65444.a4.
39. Akinosho, H.O.; Yoo, C.G.; Dumitrache, A.; Natzke, J.; Muchero, W.; Brown, S.D.; Ragauskas, A.J. Elucidating the Structural Changes to *Populus* Lignin during Consolidated Bioprocessing with *Clostridium thermocellum*. *ACS Sustain. Chem. Eng.* **2017**, *5*, 7486–7491. https://doi.org/10.1021/acssuschemeng.7b01203.
40. Chromophores in Kraft Lignin. In *Lignin Structure and Reactions*; Marton, J., Ingemar Falkehag, S., Eds.; Advances in Chemistry; American Chemical Society: Washington, DC, USA, 1966; Volume 59, ISBN 978-0-8412-0060-9.
41. Lanzalunga, O.; Bietti, M. Photo- and Radiation Chemical Induced Degradation of Lignin Model Compounds. *J. Photochem. hotobiol. B Biol.* **2000**, *56*, 85–108. https://doi.org/10.1016/S1011-1344(00)00054-3.
42. Barsberg, S.; Elder, T.; Felby, C. Lignin–Quinone Interactions: Implications for Optical Properties of Lignin. *Chem. Mater.* **2003**, *15*, 649–655. https://doi.org/10.1021/cm021162s.
43. Sadeghifar, H.; Ragauskas, A. Lignin as a UV Light Blocker—A Review. *Polymers* **2020**, *12*, 1134. https://doi.org/10.3390/polym12051134.
44. Luo, H.; Abu-Omar, M.M. Chemicals From Lignin. In *Encyclopedia of Sustainable Technologies*; Elsevier: Amsterdam, Netherlands, 2017; pp. 573–585, ISBN 978-0-12-804792-7.
45. Mandlekar, N.; Cayla, A.; Rault, F.; Giraud, S.; Salaün, F.; Malucelli, G.; Guan, J.-P. An Overview on the Use of Lignin and Its Derivatives in Fire Retardant Polymer Systems. In *Lignin—Trends and Applications*; Poletto, M., Ed.; InTech: London, UK, 2018; ISBN 978-953-51-3901-0.
46. Demuner, I.F.; Colodette, J.L.; Demuner, A.J.; Jardim, C.M. Biorefinery Review: Wide-Reaching Products through Kraft Lignin. *BioResources* **2019**, *14*, 7543–7581. https://doi.org/10.15376/biores.14.3.Demuner.
47. Strassberger, Z.; Tanase, S.; Rothenberg, G. The Pros and Cons of Lignin Valorisation in an Integrated Biorefinery. *RSC Adv.* **2014**, *4*, 25310–25318. https://doi.org/10.1039/C4RA04747H.
48. Vishtal, A.; Kraslawski, A. Challenges in Industrial Applications of Technical Lignins. *BioResources* **2011**, *6*, 3547–3568. https://doi.org/10.15376/biores.6.3.vishtal.
49. Eraghi Kazzaz, A.; Fatehi, P. Technical Lignin and Its Potential Modification Routes: A Mini-Review. *Ind. Crops Prod.* **2020**, *154*, 112732. https://doi.org/10.1016/j.indcrop.2020.112732.
50. Kumari, D.; Singh, R. Pretreatment of Lignocellulosic Wastes for Biofuel Production: A Critical Review. *Renew. Sustain. Energy Rev.* **2018**, *90*, 877–891. https://doi.org/10.1016/j.rser.2018.03.111.
51. Ab Rasid, N.S.; Shamjuddin, A.; Abdul Rahman, A.Z.; Amin, N.A.S. Recent Advances in Green Pre-Treatment Methods of Lignocellulosic Biomass for Enhanced Biofuel Production. *J. Clean. Prod.* **2021**, *321*, 129038. https://doi.org/10.1016/j.jclepro.2021.129038.
52. Matsakas, L.; Karnaouri, A.; Cwirzen, A.; Rova, U.; Christakopoulos, P. Formation of Lignin Nanoparticles by Combining Organosolv Pretreatment of Birch Biomass and Homogenization Processes. *Molecules* **2018**, *23*, 1822. https://doi.org/10.3390/molecules23071822.
53. Adamcyk, J.; Beisl, S.; Amini, S.; Jung, T.; Zikeli, F.; Labidi, J.; Friedl, A. Production and Properties of Lignin Nanoparticles from Ethanol Organosolv Liquors—Influence of Origin and Pretreatment Conditions. *Polymers* **2021**, *13*, 384. https://doi.org/10.3390/polym13030384.
54. Raj, S.; Jose, S.; Sumod, U.; Sabitha, M. Nanotechnology in Cosmetics: Opportunities and Challenges. *J. Pharm. Bioall. Sci.* **2012**, *4*, 186. https://doi.org/10.4103/0975-7406.99016.
55. Larese Filon, F.; Mauro, M.; Adami, G.; Bovenzi, M.; Crosera, M. Nanoparticles Skin Absorption: New Aspects for a Safety Profile Evaluation. *Regul. Toxicol. Pharmacol.* **2015**, *72*, 310–322. https://doi.org/10.1016/j.yrtph.2015.05.005.
56. Frangville, C.; Rutkevičius, M.; Richter, A.P.; Velev, O.D.; Stoyanov, S.D.; Paunov, V.N. Fabrication of Environmentally Biodegradable Lignin Nanoparticles. *ChemPhysChem* **2012**, *13*, 4235–4243. https://doi.org/10.1002/cphc.201200537.
57. Richter, A.P.; Bharti, B.; Armstrong, H.B.; Brown, J.S.; Plemmons, D.; Paunov, V.N.; Stoyanov, S.D.; Velev, O.D. Synthesis and Characterization of Biodegradable Lignin Nanoparticles with Tunable Surface Properties. *Langmuir* **2016**, *32*, 6468–6477. https://doi.org/10.1021/acs.langmuir.6b01088.
58. Lievonen, M.; Valle-Delgado, J.J.; Mattinen, M.-L.; Hult, E.-L.; Lintinen, K.; Kostiainen, M.A.; Paananen, A.; Szilvay, G.R.; Setälä, H.; Österberg, M. A Simple Process for Lignin Nanoparticle Preparation. *Green Chem.* **2016**, *18*, 1416–1422. https://doi.org/10.1039/C5GC01436K.
59. Ju, T.; Zhang, Z.; Li, Y.; Miao, X.; Ji, J. Continuous Production of Lignin Nanoparticles Using a Microchannel Reactor and Its Application in UV-Shielding Films. *RSC Adv.* **2019**, *9*, 24915–24921. https://doi.org/10.1039/C9RA05064G.
60. Conner, C.G.; Veleva, A.N.; Paunov, V.N.; Stoyanov, S.D.; Velev, O.D. Scalable Formation of Concentrated Monodisperse Lignin Nanoparticles by Recirculation-Enhanced Flash Nanoprecipitation. *Part. Part. Syst. Charact.* **2020**, *37*, 2000122. https://doi.org/10.1002/ppsc.202000122.
61. Ma, M.; Dai, L.; Xu, J.; Liu, Z.; Ni, Y. A Simple and Effective Approach to Fabricate Lignin Nanoparticles with Tunable Sizes Based on Lignin Fractionation. *Green Chem.* **2020**, *22*, 211–217.

62. Morsali, M.; Moreno, A.; Loukovitou, A.; Pylypchuk, I.; Sipponen, M.H. Stabilized Lignin Nanoparticles for Versatile Hybrid and Functional Nanomaterials. *Biomacromolecules* **2022**, *23*, 4597–4606. https://doi.org/10.1021/acs.biomac.2c00840.
63. Gilca, I.A.; Popa, V.I.; Crestini, C. Obtaining Lignin Nanoparticles by Sonication. *Ultrason. Sonochem.* **2015**, *23*, 369–375. https://doi.org/10.1016/j.ultsonch.2014.08.021.
64. Nair, S.S.; Sharma, S.; Pu, Y.; Sun, Q.; Pan, S.; Zhu, J.Y.; Deng, Y.; Ragauskas, A.J. High Shear Homogenization of Lignin to Nanolignin and Thermal Stability of Nanolignin-Polyvinyl Alcohol Blends. *ChemSusChem* **2014**, *7*, 3513–3520. https://doi.org/10.1002/cssc.201402314.
65. Juikar, S.J.; Vigneshwaran, N. Extraction of Nanolignin from Coconut Fibers by Controlled Microbial Hydrolysis. *Ind. Crops Prod.* **2017**, *109*, 420–425. https://doi.org/10.1016/j.indcrop.2017.08.067.
66. Garcia Gonzalez, M.N.; Levi, M.; Turri, S.; Griffini, G. Lignin Nanoparticles by Ultrasonication and Their Incorporation in Waterborne Polymer Nanocomposites: ARTICLE. *J. Appl. Polym. Sci.* **2017**, *134*, 45318. https://doi.org/10.1002/app.45318.
67. Mili, M.; Hashmi, S.A.R.; Tilwari, A.; Rathore, S.K.S.; Naik, A.; Srivastava, A.K.; Verma, S. Preparation of Nanolignin Rich Fraction from Bamboo Stem via Green Technology: Assessment of Its Antioxidant, Antibacterial and UV Blocking Properties. *Environ. Technol.* **2023**, *44*, 416–430. https://doi.org/10.1080/09593330.2021.1973574.
68. Abbati de Assis, C.; Greca, L.G.; Ago, M.; Balakshin, M.Y.; Jameel, H.; Gonzalez, R.; Rojas, O.J. Techno-Economic Assessment, Scalability, and Applications of Aerosol Lignin Micro- and Nanoparticles. *ACS Sustain. Chem. Eng.* **2018**, *6*, 11853–11868. https://doi.org/10.1021/acssuschemeng.8b02151.
69. Hussin, M.H.; Appaturi, J.N.; Poh, N.E.; Latif, N.H.A.; Brosse, N.; Ziegler-Devin, I.; Vahabi, H.; Syamani, F.A.; Fatriasari, W.; Solihat, N.N.; et al. A Recent Advancement on Preparation, Characterization and Application of Nanolignin. *Int. J. Biol. Macromol.* **2022**, *200*, 303–326. https://doi.org/10.1016/j.ijbiomac.2022.01.007.
70. Tan, S.; Liu, D.; Qian, Y.; Wang, J.; Huang, J.; Yi, C.; Qiu, X.; Qin, Y. Towards Better UV-Blocking and Antioxidant Performance of Varnish via Additives Based on Lignin and Its Colloids. *Holzforschung* **2019**, *73*, 485–491. https://doi.org/10.1515/hf-2018-0134.
71. Girard, V.; Chapuis, H.; Brosse, N.; Canilho, N.; Marchal-Heussler, L.; Ziegler-Devin, I. Lignin Nanoparticles: Contribution of Biomass Types and Fractionation for an Eco-Friendly Production. *ACS Sustain. Chem. Eng.* **2024**, *12*, 7055–7068. https://doi.org/10.1021/acssuschemeng.4c00711.
72. El Hage, R.; Brosse, N.; Chrusciel, L.; Sanchez, C.; Sannigrahi, P.; Ragauskas, A. Characterization of Milled Wood Lignin and Ethanol Organosolv Lignin from Miscanthus. *Polym. Degrad. Stab.* **2009**, *94*, 1632–1638. https://doi.org/10.1016/j.polymdegradstab.2009.07.007.
73. Steinmetz, V.; Villain-Gambier, M.; Klem, A.; Gambier, F.; Dumarcay, S.; Trebouet, D. Unveiling TMP Process Water Potential As an Industrial Sourcing of Valuable Lignin–Carbohydrate Complexes toward Zero-Waste Biorefineries. *ACS Sustain. Chem. Eng.* **2019**, *7*, 6390–6400. https://doi.org/10.1021/acssuschemeng.9b00181.
74. He, Q.; Ziegler-Devin, I.; Chrusciel, L.; Obame, S.N.; Hong, L.; Lu, X.; Brosse, N. Lignin-First Integrated Steam Explosion Process for Green Wood Adhesive Application. *ACS Sustain. Chem. Eng.* **2020**, *8*, 5380–5392. https://doi.org/10.1021/acssuschemeng.0c01065.
75. Zhang, J.; Tian, Z.; Ji, X.-X.; Zhang, F. Light-Colored Lignin Extraction by Ultrafiltration Membrane Fractionation for Lignin Nanoparticles Preparation as UV-Blocking Sunscreen. *Int. J. Biol. Macromol.* **2023**, *231*, 123244. https://doi.org/10.1016/j.ijbiomac.2023.123244.
76. Sayre, R.M.; Agin, P.P.; LeVee, G.J.; Marlowe, E. A Comparison of in Vivo and in Vitro Testing of Sunscreening Formulas. *Photochem. Photobiol.* **1979**, *29*, 559–566. https://doi.org/10.1111/j.1751-1097.1979.tb07090.x.
77. Brosse, N.; El Hage, R.; Chaouch, M.; Pétrissans, M.; Dumarçay, S.; Gérardin, P. Investigation of the Chemical Modifications of Beech Wood Lignin during Heat Treatment. *Polym. Degrad. Stab.* **2010**, *95*, 1721–1726. https://doi.org/10.1016/j.polymdegradstab.2010.05.018.
78. Siika-aho, M.; Varhimo, A.; Sirviö, J.; Kruus, K. Sugars from Biomass—High Cellulose Hydrolysability of Oxygen Alkali Treated Spruce, Beech and Wheat Straw. In Proceedings of the 6th NordicWood Biorefinery Conference 2015 (NWBC), Helsinki, Finland, 20–22 October 2015, ISBN 978-951-38-8352-2.
79. Schneider, W.D.H.; Dillon, A.J.P.; Camassola, M. Lignin Nanoparticles Enter the Scene: A Promising Versatile Green Tool for Multiple Applications. *Biotechnol. Adv.* **2021**, *47*, 107685. https://doi.org/10.1016/j.biotechadv.2020.107685.
80. Pylypchuk, I.V.; Riazanova, A.; Lindström, M.E.; Sevastyanova, O. Structural and Molecular-Weight-Dependency in the Formation of Lignin Nanoparticles from Fractionated Soft- and Hardwood Lignins. *Green Chem.* **2021**, *23*, 3061–3072. https://doi.org/10.1039/D0GC04058D.
81. Zwilling, J.D.; Jiang, X.; Zambrano, F.; Venditti, R.A.; Jameel, H.; Velev, O.D.; Rojas, O.J.; Gonzalez, R. Understanding Lignin Micro- and Nanoparticle Nucleation and Growth in Aqueous Suspensions by Solvent Fractionation. *Green Chem.* **2021**, *23*, 1001–1012. https://doi.org/10.1039/D0GC03632C.
82. Tian, D.; Hu, J.; Chandra, R.P.; Saddler, J.N.; Lu, C. Valorizing Recalcitrant Cellulolytic Enzyme Lignin via Lignin Nanoparticles Fabrication in an Integrated Biorefinery. *ACS Sustain. Chem. Eng.* **2017**, *5*, 2702–2710. https://doi.org/10.1021/acssuschemeng.6b03043.
83. Ma, Y.; Liao, Y.; Jiang, Z.; Sun, Q.; Guo, X.; Zhang, W.; Hu, C.; Luque, R.; Shi, B.; Sels, B.F. Solvent Effect on the Production of Spherical Lignin Nanoparticles. *Green Chem.* **2023**, *25*, 993–1003. https://doi.org/10.1039/D2GC04014J.
84. Zhang, Y.; Naebe, M. Lignin: A Review on Structure, Properties, and Applications as a Light-Colored UV Absorber. *ACS Sustain. Chem. Eng.* **2021**, *9*, 1427–1442. https://doi.org/10.1021/acssuschemeng.0c06998.

85. Guo, Y.; Tian, D.; Shen, F.; Yang, G.; Long, L.; He, J.; Song, C.; Zhang, J.; Zhu, Y.; Huang, C.; et al. Transparent Cellulose/Technical Lignin Composite Films for Advanced Packaging. *Polymers* **2019**, *11*, 1455. https://doi.org/10.3390/polym11091455.
86. Xie, M.; Chen, Z.; Xia, Y.; Lin, M.; Li, J.; Lan, W.; Zhang, L.; Yue, F. Influence of the Lignin Extraction Methods on the Content of Tricin in Grass Lignins. *Front. Energy Res.* **2021**, *9*, 756285. https://doi.org/10.3389/fenrg.2021.756285.
87. Lim, J.; Sana, B.; Krishnan, R.; Seayad, J.; Ghadessy, F.J.; Jana, S.; Ramalingam, B. Laccase-Catalyzed Synthesis of Low-Molecular-Weight Lignin-Like Oligomers and Their Application as UV-Blocking Materials. *Chemistry* **2018**, *13*, 284–291. https://doi.org/10.1002/asia.201701573.
88. Yearla, S.R.; Padmasree, K. Preparation and Characterisation of Lignin Nanoparticles: Evaluation of Their Potential as Antioxidants and UV Protectants. *J. Exp. Nanosci.* **2016**, *11*, 289–302. https://doi.org/10.1080/17458080.2015.1055842.
89. Auxenfans, T.; Crônier, D.; Chabbert, B.; Paës, G. Understanding the Structural and Chemical Changes of Plant Biomass Following Steam Explosion Pretreatment. *Biotechnol Biofuels* **2017**, *10*, 36. https://doi.org/10.1186/s13068-017-0718-z.